



OPEN Multi-omic analyses reveal PTPN6's impact on tumor immunity across various cancers

Yuchen Zhong^{1,2,3,4}, Weiyuan Zhang^{1,4}, Chaojing Zheng^{1,2}, Hongyu Wu², Jun Luo^{1,2}, Ziming Yuan¹, Hao Zhang¹, Chunlin Wang¹, Haiyang Feng², Meng Wang², Qian Zhang²✉, Haixing Ju²✉ & Guiyu Wang¹✉

Protein Tyrosine Phosphatase Non-Receptor Type 6 (PTPN6) plays a crucial regulatory role in cellular processes and has been implicated in oncogenesis. This pan-cancer analysis aimed to elucidate PTPN6's involvement across various cancer types, with a particular emphasis on its association with tumor immunity. We analyzed PTPN6 expression data from open access databases using various statistical techniques, including survival analysis, genetic heterogeneity analysis, immune profiling, single-cell analysis, drug sensitivity analysis, and protein interaction analysis. We also conducted in vitro experiments utilizing colorectal cancer cell lines to validate PTPN6's functional role. PTPN6 exhibited distinct expression patterns across cancers, and its prognostic significance was apparent in several cancer types, particularly in glioblastoma, sarcoma, and melanoma. We observed correlations between PTPN6 and immune genes/cell infiltration in these cancers, suggesting a potential role in modulating the tumor immune microenvironment. Single-cell analysis revealed that PTPN6 is predominantly localized in macrophages, B cells, and dendritic cells within the tumor microenvironment, implying its involvement in regulating immune cell function. Enrichment analysis highlighted PTPN6's role in immune-related pathways. Drug sensitivity analysis identified specific drugs, including PAC-1, SNX-2112, BELINOSTAT, VORINOSTAT, TPCA-1, and PHA-893,888, whose efficacy may be influenced by PTPN6 expression. Knocking down PTPN6 expression inhibited the proliferation and migration of colorectal cancer cells in vitro, confirming its oncogenic role in this cancer type. This pan-cancer analysis establishes PTPN6's multifaceted influence on tumor immunity and its potential as a biomarker and therapeutic target.

Abbreviations

ACC	Adrenocortical carcinoma
AEL	Acute erythroid leukemia
AML	Acute myeloid leukemia
ALL	Acute lymphoblastic leukemia
BCC	Basal cell carcinoma
BLCA	Bladder urothelial carcinoma
BRCA	Breast invasive carcinoma
CESC	Cervical squamous cell carcinoma and endocervical adenocarcinoma
CHOL	Cholangiocarcinoma
CLL	Chronic lymphocytic leukemia
COAD	Colon adenocarcinoma
COADREAD/COREAD	Colon adenocarcinoma/rectum adenocarcinoma esophageal carcinoma
CRC	Colorectal cancer
DLBC	Lymphoid neoplasm diffuse large B-cell lymphoma
ESCA	Esophageal carcinoma

¹Department of Colorectal Cancer Surgery, the Second Affiliated Hospital of Harbin Medical University, Harbin 150000, Heilongjiang, People's Republic of China. ²Department of Colorectal Cancer Surgery, Zhejiang Cancer Hospital, Hangzhou Institute of Medicine (HIM), Chinese Academy of Sciences, Hangzhou, Zhejiang, People's Republic of China. ³Cancer Center, Department of Medical Oncology, Zhejiang Provincial People's Hospital (Affiliated People's Hospital), Hangzhou Medical College, Hangzhou, Zhejiang, People's Republic of China. ⁴Yuchen Zhong and Weiyuan Zhang contributed equally to this work. ✉email: zhangqian1171@126.com; juhx@zjcc.org.cn; guiyuwang@hrbmu.edu.cn

GCTB	Giant cell tumor of bone
GBM	Glioblastoma multiforme
GBMLGG	Glioma
GIST	Gastrointestinal stromal tumor
HNSC	Head and neck squamous cell carcinoma
KICH	Kidney chromophobe
KIPAN	Pan-kidney cohort (KICH + KIRC + KIRP)
KIRC	Kidney renal clear cell carcinoma
KIRP	Kidney renal papillary cell carcinoma
LAML	Acute myeloid leukemia
LGG	Brain lower grade glioma
LIHC	Liver hepatocellular carcinoma
LUAD	Lung adenocarcinoma
LUSC	Lung squamous cell carcinoma
LSCC	Laryngeal squamous cell carcinoma
MB	Medulloblastoma
MCC	Merkel cell carcinoma
MESO	Mesothelioma
MF	Mycosis fungoides
MM	Multiple myeloma
MPNST	Malignant peripheral nerve sheath tumor
NB	Neuroblastoma
NHL	Non-Hodgkin lymphoma
NPC	Nasopharyngeal carcinoma
OV	Ovarian serous cystadenocarcinoma
OS	Osteosarcoma
OSCC	Oral squamous cell carcinoma
PAAD	Pancreatic adenocarcinoma
PBMC	Peripheral blood mononuclear cell
PCFCL	Primary cutaneous follicle center lymphoma
PCPG	Pheochromocytoma and paraganglioma
PRAD	Prostate adenocarcinoma
READ	Rectum adenocarcinoma
SARC	Sarcoma
STAD	Stomach adenocarcinoma
SKCM	Skin cutaneous melanoma
SCC	Squamous cell carcinoma
SCLC	Small cell lung cancer
STES	Stomach and esophageal carcinoma
SS	Synovial sarcoma
TGCT	Testicular germ cell tumors
THCA	Thyroid carcinoma
THYM	Thymoma
UCEC	Uterine corpus endometrial carcinoma
UCS	Uterine carcinosarcoma
UVM	Uveal melanoma
WT	High-risk wilms tumor

Protein Tyrosine Phosphatase Non-Receptor Type 6 (PTPN6) is a member of the protein tyrosine phosphatase (PTP) family, which regulates cellular signaling pathways involved in various processes such as cell growth, differentiation, mitotic cycle, and oncogenic transformation. These enzymes are critical signaling molecules in cellular communication. PTPN6 plays a pivotal regulatory role in the inflammatory process¹. In PTPN6 knockout mice, inflammatory cytokine levels in leukocytes are significantly elevated, accompanied by a systemic increase in inflammation². Mechanistically, PTPN6 enhances the regulatory function of receptor-interacting protein kinases, suppresses receptor-interacting serine/threonine-protein kinase 3 (RIPK3)- and mixed lineage kinase domain-like protein (MLKL)-dependent necroptosis, inhibits caspase-8-dependent apoptosis, and downregulates the activation of the p38/mitogen-activated protein kinase (MAPK) signaling pathway^{2–6}. PTPN6 regulates protein-tyrosine phosphorylation/dephosphorylation and is involved in cellular processes such as proliferation, differentiation, survival, migration, and invasion⁷. PTPN6, encoding SHP1, consists of 17 exons and features two SH2 domains essential for binding phosphorylated tyrosine residues on target proteins⁸. SHP1, a non-receptor tyrosine phosphatase, is involved in numerous signaling pathways and can be inhibited by protein kinase C α -mediated phosphorylation at Ser591 in its C-terminal region⁹. It dephosphorylates substrates in signaling cascades mediated by Src-family kinases (SFKs) and spleen tyrosine kinase (SYK)¹⁰.

Current study concluded that PTPN6 is closely associated with the prognosis of neuroblastoma¹¹. PTPN6 may also play a regulatory role in hematological cancers, and PTPN6 may be involved in the progression of chronic myeloid leukaemia with DNA methylation, in diffuse large B-cell lymphoma, mutated PTPN6 reduced tyrosine phosphatase activity and exhibited enhanced STAT3 transactivation activity^{12,13}. In human epithelial ovarian cancer, the aberrant expression of PTPN6 has been demonstrated¹⁴. In colorectal cancer, previous studies have indicated that PTPN6 can form a complex with EGFR and promote colorectal carcinogenesis and

metastasis, while other study have found that PTPN6 interacts with the MAPK signaling pathway and affects the sensitivity of chemotherapy^{15,16}. A recent study using single-cell sequencing revealed that PTPN6 is closely associated with immune suppression in glioblastoma¹⁷.

In breast cancer, PTPN6 acts as a tumor suppressor by binding to EGFR and dephosphorylating S6A3^{18,19}. In hepatocellular carcinoma, PTPN6 plays a role in inhibiting epithelial-mesenchymal transition (EMT) primarily by suppressing TGF- β 1, thereby reducing p-S6A3 levels and attenuating the process of epithelial-mesenchymal transition^{20,21}.

In lung cancer, PTPN6 may also exhibit anticancer effects by inactivating the PI3K/AKT signaling pathway to suppress the development of lung cancer²². Additionally, the outcome of radiation therapy in lung cancer has been associated with PTPN6²³. In summary, PTPN6 plays varying roles in different cancer types but primarily functions as a tumor suppressor, exerting anticancer effects.

PTPN6 is closely associated with tumor immunity, and in the context of lung cancer, the PTPN6 axis counteracts adaptive immune evasion²⁴. PTPN6 itself serves as a dendritic cells (DC) intrinsic checkpoint and plays a crucial role in tumor immunity. PTPN6 can facilitate tumor-associated DCs to uptake immune complexes, thereby inducing tumor immune responses²⁵. PTPN6 also plays a critical role in the functioning of NK cells, contributing to NK cell tolerance and education²⁶.

In summary, PTPN6 plays important roles in multiple pathways and exhibits a dual function in cancer, particularly in relation to tumor immunity. Despite its significant roles, research on PTPN6 across various cancer types remains sparse. Currently, comprehensive pan-cancer analysis articles on PTPN6 are lacking. By leveraging publicly available databases such as TCGA, it is hoped that a systematic pan-cancer analysis of PTPN6 can be conducted. Such studies would significantly enhance our understanding of its involvement and functions in different cancer types.

Result

Aberrant expression of PTPN6 in cancer

Aberrant expression of PTPN6 in cancer has been observed, where its expression levels can be either upregulated or downregulated depending on the cancer type. Such dysregulated expression can have significant implications for cancer development and progression. We initially compared the expression levels of PTPN6 between cancer and normal tissues using TCGA data. The results revealed that PTPN6 exhibited significantly higher expressions in LGG, LIHC, GBM, PRAD, HNSC, ESCA, STAD, KIRC, BRCA, CHOL, UCEC, KIRP, and BLCA, while showing significantly lower expression in KICH, LUAD, and LUSC (Fig. 1A). However, considering the limited sample size of normal tissues in TCGA, we performed a comparison after integrating TCGA with GTEx data. As shown in Fig. 1B, aberrantly high expression of PTPN6 was observed in LGG, UCS, LIHC, GBM, HNSC, ESCA, STAD, COADREAD, OV, KIRC, BRCA, THCA, CHOL, UCEC, PRAD, KIRP, CESC, BLCA, TGCT, and LAML. Conversely, abnormal low expression was observed in WT, LUSC, LUAD, and ALL. No statistically significant differences were found in ACC, KICH, PCPG, and PRAD. In Fig. 1C, the expression levels of PTPN6 across various cell lines are shown. We found that PTPN6 is most highly expressed in leukemia, myeloma, and lymphoma cell lines, while it is almost undetectable in liposarcoma.

The expression of PTPN6 is associated with cancer prognosis

We performed survival analysis using the TCGA database, categorizing patients with various types of cancer into two groups based on the median expression level of PTPN6. As shown in Fig. 2A, we observed that high expression of PTPN6 was associated with poorer prognosis in COADREAD, KIRC, LAML, LGG, and UVM. Conversely, in BLCA, SKCM, LUAD, CESC, BRCA, SARC, MESO, PAAD, and STAD, high expression of PTPN6 was associated with longer overall survival. Moreover, we observed that in COADREAD, the hazard ratio reached 2.11, indicating a significant impact of PTPN6 on prognosis in COADREAD. Consistent with previous studies, high expression of PTPN6 was found to be a favorable prognostic factor in BRCA and LUAD^{27,28}.

Similar findings were observed in the analysis of PTPN6 and DSS (Disease-Specific Survival). In KIRC, LGG, UVM, and COADREAD, high expression of PTPN6 was associated with an increased risk of poor prognosis. Conversely, in BLCA, SKCM, LUAD, CESC, MESO, SARC, and PAAD, high expression of PTPN6 was identified as a protective factor for prognosis (Fig. 2B).

Furthermore, we employed the optimal cutoff algorithm to analyze the relationship between PTPN6 expression and overall survival. Supplementary Fig. 1 presents the Kaplan-Meier survival curves for different cancers. Overall, PTPN6 was identified as a favorable prognostic factor in most cancers, including ACC, BLCA, BRCA, KIRP, PAAD, LUAD, SARC, MESO, THYM, STAD, and SKCM (Supplementary Fig. 1A). However, in COADREAD, LGG, GBM, LAML, KIRC, and UVM, patients with high PTPN6 expression exhibited significantly shorter survival times (Supplementary Fig. 1B). Following the methodology of previous study²⁹, we utilized the MethSurv platform to analyze the relationship between PTPN6 methylation and survival across various cancers. As shown in Supplementary Table 1, we found that in ACC, BLCA, COAD, HNSC, KIRP, LAML, MESO, and UCEC, PTPN6 methylation is associated with a significant increase in patient survival risk. Conversely, in GBM, KIRC, LGG, SARC, STAD, and UVM, changes in PTPN6 methylation are associated with a significant decrease in survival risk.

Correlation analysis revealed significant negative associations between PTPN6 methylation and mRNA expression in most cancer types (Supplementary Table 2). Strong negative correlations were observed in cancers such as ACC ($R = -0.722$, $FDR = 0$), KIRC ($R = -0.657$, $FDR = 0$), SKCM ($R = -0.834$, $FDR = 0$), and UVM ($R = -0.868$, $FDR = 0$). Other cancers, including LIHC ($R = -0.448$, $FDR = 0$) and LUAD ($R = -0.429$, $FDR = 0$), also demonstrated significant correlations. By contrast, weaker or nonsignificant correlations were noted in a few cancer types, such as DLBC ($R = -0.191$, $FDR = 0.194$). Overall, these results suggest that PTPN6 methylation

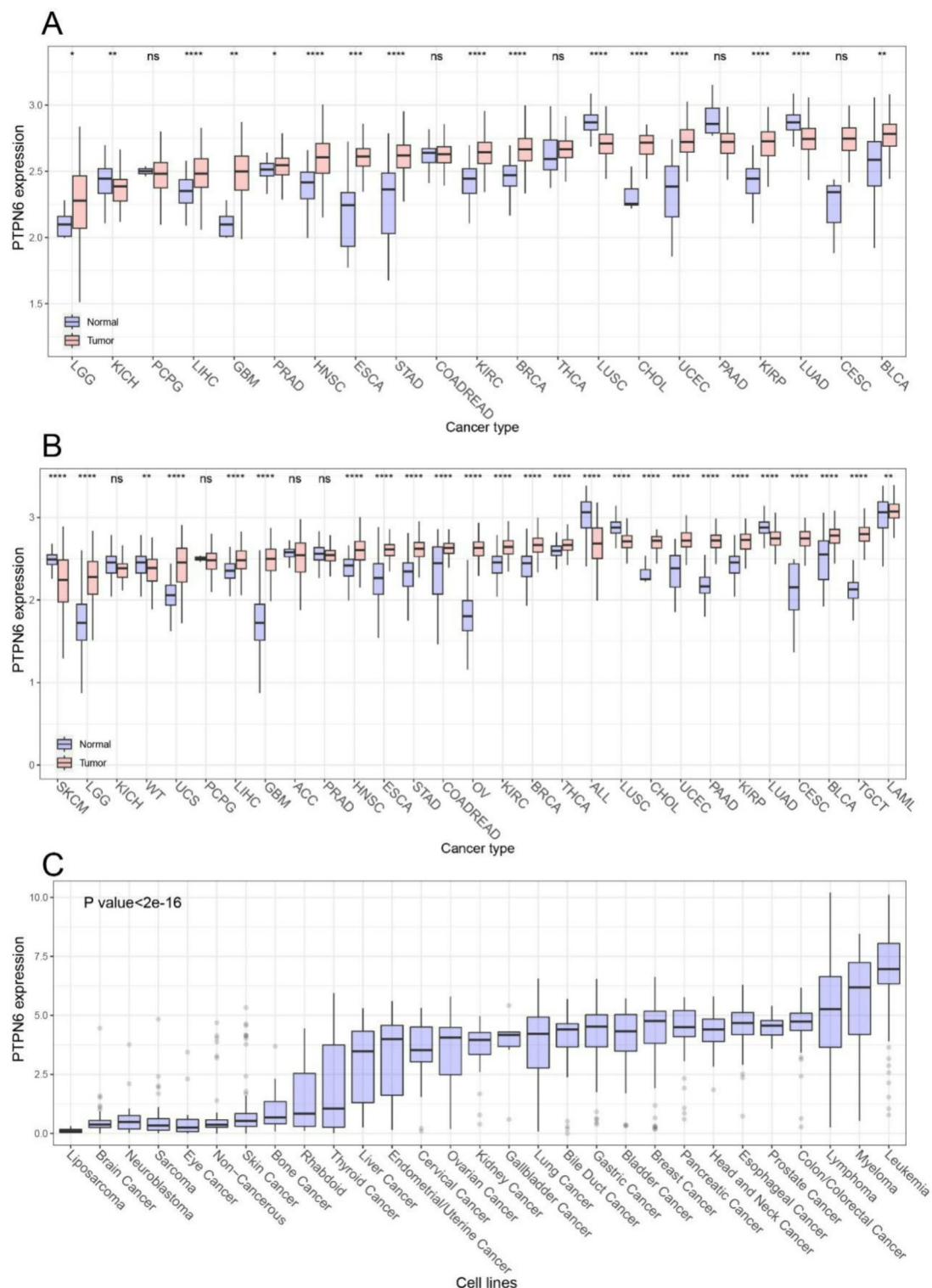


Fig. 1. Expression patterns of PTPN6 across cancers, normal tissues, and cell lines. **(A)** Box plots comparing PTPN6 expression in tumor samples from TCGA and matched normal tissue samples; **(B)** PTPN6 expression distributions in tumors from TCGA and normal samples from GTEx across cancer types; **(C)** PTPN6 expression levels across different cancer cell lines from the Cancer Cell Line Encyclopedia (CCLE). Statistical significance: * $p < 0.05$, ** $p < 0.01$, *** $p < 0.001$, **** $p < 0.0001$, ns represents Not significant.

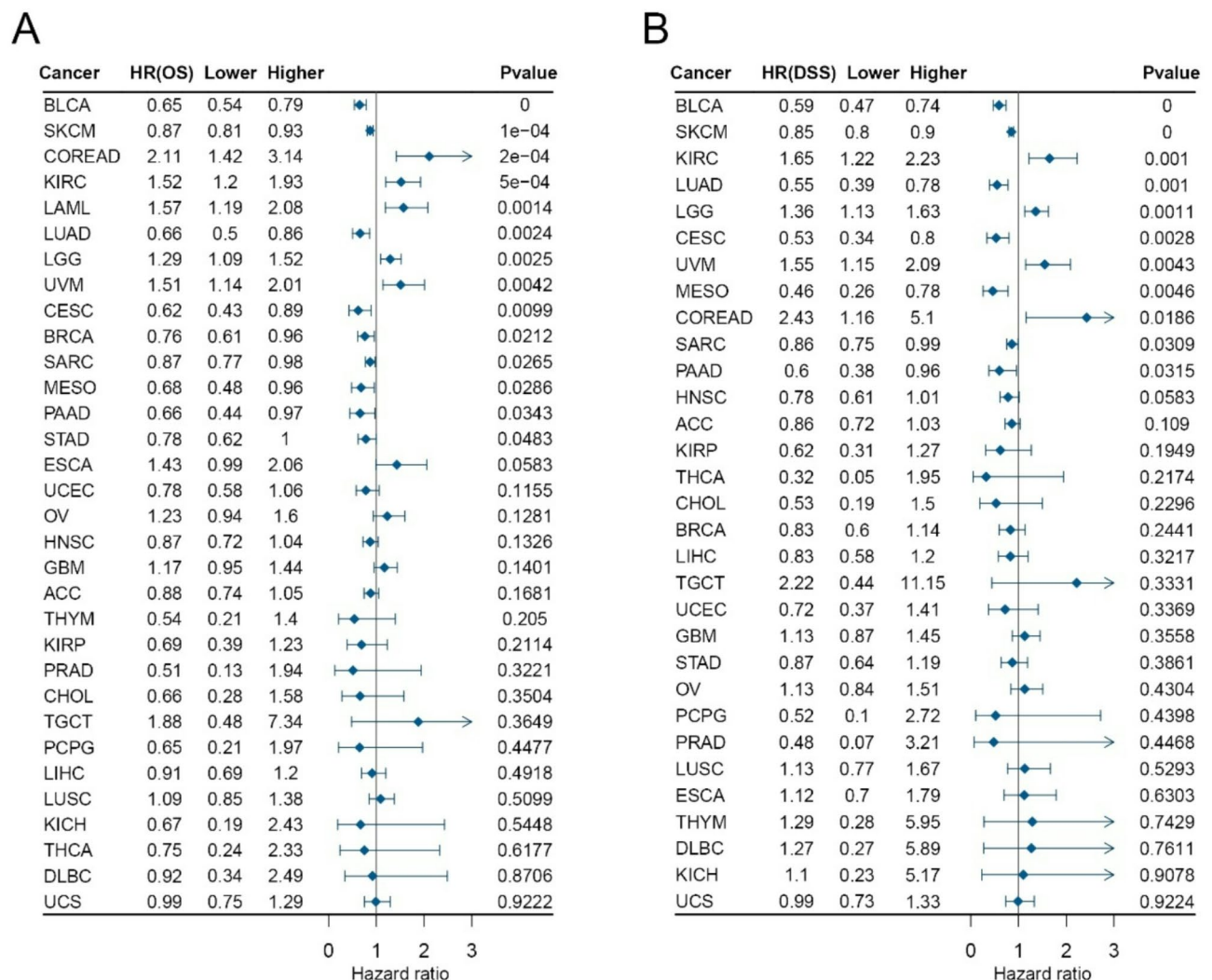


Fig. 2. Association between PTPN6 expression and patient survival outcomes. (A) Forest plot depicting the hazard ratios and 95% confidence intervals for the correlation between PTPN6 expression and overall survival across cancer types; (B) Forest plot showing the hazard ratios and 95% confidence intervals for the relationship between PTPN6 expression and disease-specific survival in different cancers.

is inversely correlated with its mRNA expression in most cancers, indicating a potential epigenetic regulatory mechanism.

The correlation between PTPN6 and immune genes

Building on previous research that underscores the close association between PTPN6 and tumor immunity and recognizing the profound influence of the immune system on tumor development, progression, and treatment, we conducted an analysis of the correlation between PTPN6 expression and immune genes in multiple types of cancer^{30,31}. In Fig. 3, we examined the correlation between PTPN6 and immune inhibitor, immune stimulator, MHC, chemokines, and immune checkpoint genes. The majority of cancers showed statistically significant positive correlations were observed. Specifically, Fig. 3A and B illustrate the correlations between PTPN6 and genes associated with immune suppression and stimulation, respectively. In GBM, LGG, and UVM, PTPN6 exhibited strong correlations with various immune genes. Interestingly, in OV, PTPN6 showed positive correlations with all immunoinhibitor. On the other hand, VTCN1, KDR, and TFGBR1 demonstrated negative correlations with PTPN6 in THYM, TGCT, BRCA, UCEC, and BLCA. In line with recent research findings, we also evaluated the correlation between PTPN6 and MHC-related genes (Fig. 3C)²⁶. Surprisingly, our analysis revealed a significant positive correlation between PTPN6 and MHC genes across almost all studied cancer types. Only in CHOL, THYM, and DLBC, the trend was either not significant or showed a negative correlation. The strongest positive correlation trends were observed in UVM, GBM, LGG, SKCM, and SARC. Chemokines play a crucial role in the immune microenvironment of cancer and are potential therapeutic targets for immunotherapy, deserving more attention³². Therefore, to further explore the immune regulatory role of PTPN6, we analyzed the correlation between it and numerous chemokine-related genes. As illustrated in

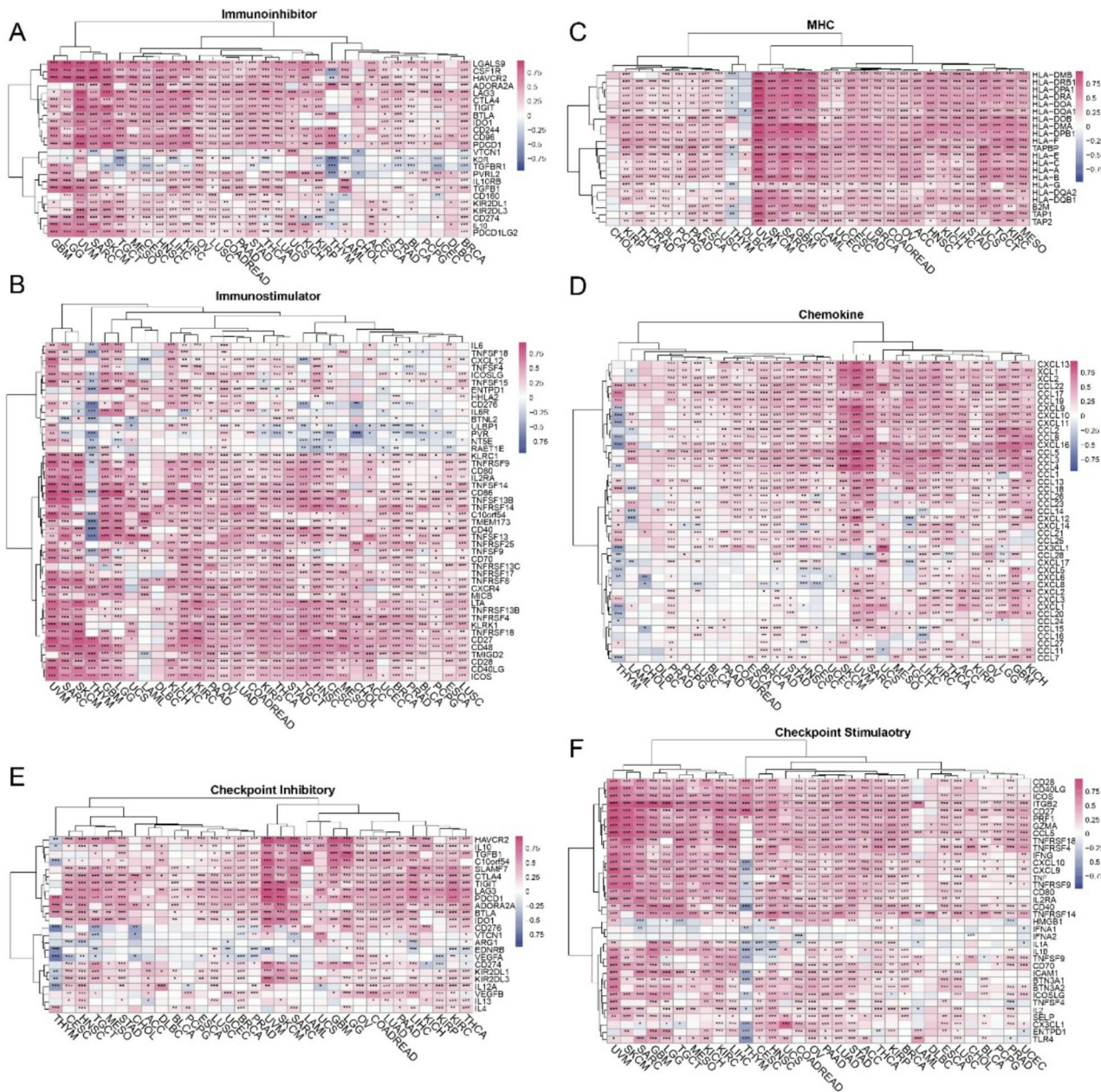


Fig. 3. Correlation analysis between PTPN6 and immune-related genes. Heatmaps depicting Pearson's correlation coefficients (R values) between PTPN6 expression and the expression of (A) immunoinhibitory genes, (B) immunostimulatory genes (C) major histocompatibility complex (MHC) genes (D) Chemokines (E) immune checkpoint inhibitors and (F) immune checkpoint stimulatory genes across cancer types. Bars denote correlation coefficient R values, * $p < 0.05$, ** $p < 0.01$, *** $p < 0.001$.

Fig. 3D, our findings demonstrate that PTPN6 generally maintained a positive correlation with chemokine genes across various cancer types, reinforcing its potential as a key player in the immune response within the tumor microenvironment. However, a few negative correlations were observed in THYM, CHOL, HNSC, CESC, and LAML.

The development of checkpoint inhibitors, such as immune checkpoint blockade therapies, has revolutionized cancer treatment. These inhibitors work by blocking the interactions between immune checkpoint proteins and their corresponding receptors, thus releasing the brakes on the immune system, and allowing it to mount a stronger and more effective anti-tumor response^{33,34}. By examining the correlation with checkpoint genes, trends still exist in tumors such as UVM, GBM, LGG, SKCM, and SARC, there is a significant positive correlation (Fig. 3E and F). However, in THYM and CHOL, the correlation is negative or not statistically significant. Moreover, among checkpoint stimulatory genes, the correlation between HMGB, IFNA1, IFNA2, and PTPN6 is extremely weak.

The protein tyrosine phosphatase PTPN6 demonstrates a robust association with immune-related genes across multiple tumor types, with notable exceptions being THYM and TGCT. This implies potential alternative functional roles for PTPN6 in THYM and TGCT pathogenesis, meriting further scholarly inquiry. Conversely, strong correlations between PTPN6 and various immune genes are observed in UVM, LGG, and GBM. These correlations suggest PTPN6 may play an integral role modulating anti-tumor immunity within the microenvironment of these malignancies. Additional investigation of PTPN6 as a prospective immunotherapeutic target in UVM, LGG, and GBM is therefore warranted based on these correlative data.

The relationship between PTPN6 and the tumor microenvironment and immune cell infiltration

The tumor microenvironment and immune cell infiltration are pivotal factors influencing tumor development. To accurately assess the level of immune infiltration in tumors, various computational algorithms are utilized. In our study, we employed four distinct algorithms to analyze the relationship between PTPN6 expression and immune cell infiltration across different cancer types. This multi-algorithm approach allowed us to comprehensively evaluate and validate the consistency of PTPN6's impact on the immune contexture of tumors.

In Supplementary Fig. 2A, the correlation between PTPN6 and three scores from the ESTIMATE algorithm is presented. PTPN6 exhibits a strong correlation with ESTIMATE score, Immune score, and stroma score in GBM, SARC, SKCM, LGG, and UVM. Interestingly, in all types of cancer, the expression level of PTPN6 shows a statistically significant positive correlation with the immune score. Supplementary Figs. 2B–D depict the correlation between PTPN6 and the MCP counter, EPIC, and Timer algorithms, respectively. Multiple algorithms revealed a significant positive correlation between PTPN6 and T cells and B cells, notably in UVM, SARC, SKCM, MESO, BRCA, PAAD, and PRAD. The MCP counter and Timer algorithms showed consistent results. However, discrepancies were noted among the algorithms; For example, EPIC algorithm indicated a negative correlation between PTPN6 and CD8 + T cells in GBM, contrasting with positive correlations observed in both the Timer and MCP counter algorithms. This discrepancy among the algorithms may be attributed to the different gene signatures each uses. Overall, the analysis indicates that PTPN6 generally shows a positive correlation with immune cell infiltration in most cancers. Additionally, it is more likely to exhibit a negative correlation with stromal cells. Notably, in UVM, GBM, LGG, and SKCM, the correlation between PTPN6 and immune cells is particularly strong. These findings highlight the potential significance of PTPN6 in regulating immune cell infiltration and underscore the need for further research and investigation specifically in these tumor types.

PTPN6 mutations and tumor heterogeneity

We conducted further analysis on the mutation status of PTPN6 across different cancers and observed that the overall mutation rate of PTPN6 is relatively low. In seminoma and ovarian epithelial tumors, amplification is the predominant type of mutation, with a mutation frequency of approximately 6%. However, in ocular melanoma, thyroid cancer, leukemia, renal cell cancer, pheochromocytoma, and cholangiocarcinoma, the mutation frequency of PTPN6 was found to be zero (Fig. 4A). Furthermore, we analyzed the copy number variation (CNV) status of PTPN6. As shown in Fig. 4B, in TGCT, the CNV mutation rate of PTPN6 is as high as 98%, primarily consisting of heterozygous amplification, with an additional 20% exhibiting homozygous amplification. In other tumors, heterozygous amplification and heterozygous deletion are the predominant CNV patterns. The proportion of homozygous deletion is extremely low, accounting for only over 1.5% in ESCA, LUSC, and HNSC, with percentages of 2.17%, 1.59%, and 1.53%, respectively. Interestingly, a significant negative correlation between PTPN6 expression and CNV was found only in TGCT. In contrast, in OV, LUSC, LUAD, ESCA, KIRP, STAD, BRCA, HNSC, READ, CESC, SKCM, KICH, LIHC, KIRC, UCEC, and PRAD, there is a statistically significant positive correlation between PTPN6 and CNV.

Further analysis was conducted to assess the correlation between PTPN6 and tumor heterogeneity. Figure 4C and F present radar plots depicting the correlation between PTPN6 expression and MSI (microsatellite instability), TMB (tumor mutational burden), MATH (mutant-allele tumor heterogeneity), and tumor purity, respectively. The correlation between PTPN6 and tumor MSI is relatively weak. It is negatively correlated with MSI in UCEC and TGCT, while positively correlated with MSI in PRAD and THCA. In other tumors, no statistically significant correlation is observed (Fig. 4C). Similarly, the correlation between TMB and PTPN6 is not significant, exhibiting a negative correlation in ACC and GBM, and a positive correlation is observed in KIRP (Fig. 4D). MATH, representing tumor heterogeneity, also shows limited correlations demonstrating a negative correlation in THYM, LUAD, STAD, THCA, and PRAD, and only a positive correlation in CHOL (Fig. 4E). Lastly, we analyzed the correlation between PTPN6 and tumor purity (Fig. 4F), which represents the tumor's immune microenvironment. In most tumors, higher PTPN6 expression is associated with lower tumor purity, consistent with the results of immune microenvironment analysis. In several types of tumors such as SARC, SKCM, GBM, THYM, TGCT, and UVM, the correlation between PTPN6 and tumor purity is lower than -0.5 and statistically significant. This indicates that higher expression of PTPN6 is associated with higher content of other cells within the tumor and potentially a higher degree of immune infiltration.

Enrichment analysis

Next, we conducted an enrichment analysis for PTPN6 by calculating differential gene expression across various cancer types, distinguished by high and low expression levels of PTPN6. Initially, a KEGG analysis was performed to explore differences in gene expression associated with high and low PTPN6 levels. We observed significant enrichment of various immune pathways, including the PD1/PDL1 pathway, leukocyte migration, immune cell differentiation, T cell and B cell signaling pathways, NK cells, as well as enrichment in chemokine and cytokine signaling pathways (Fig. 5A).

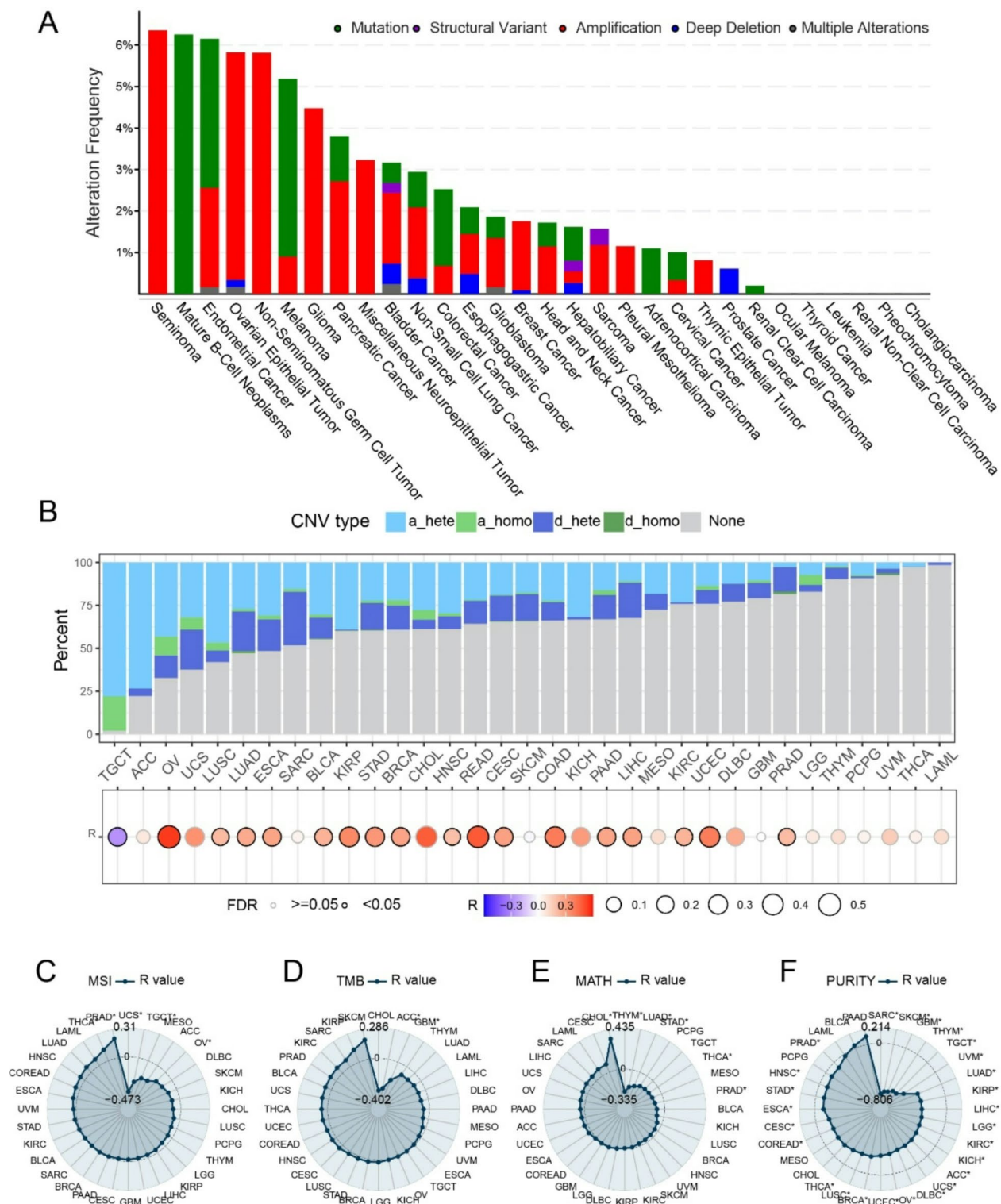


Fig. 4. PTPN6 mutations and associations with tumor heterogeneity. **(A)** Stacked bar chart showing the frequency of PTPN6 mutations across different cancer types; **(B)** PTPN6 CNV mutations and correlation between CNV and gene expression; Radar charts depicting the correlation between PTPN6 expression and **(C)** microsatellite instability (MSI) scores, **(D)** tumor mutational burden (TMB) scores, **(E)** mutant-allele tumor heterogeneity (MATH) scores, and **(F)** tumor purity across cancers. * $p < 0.05$.

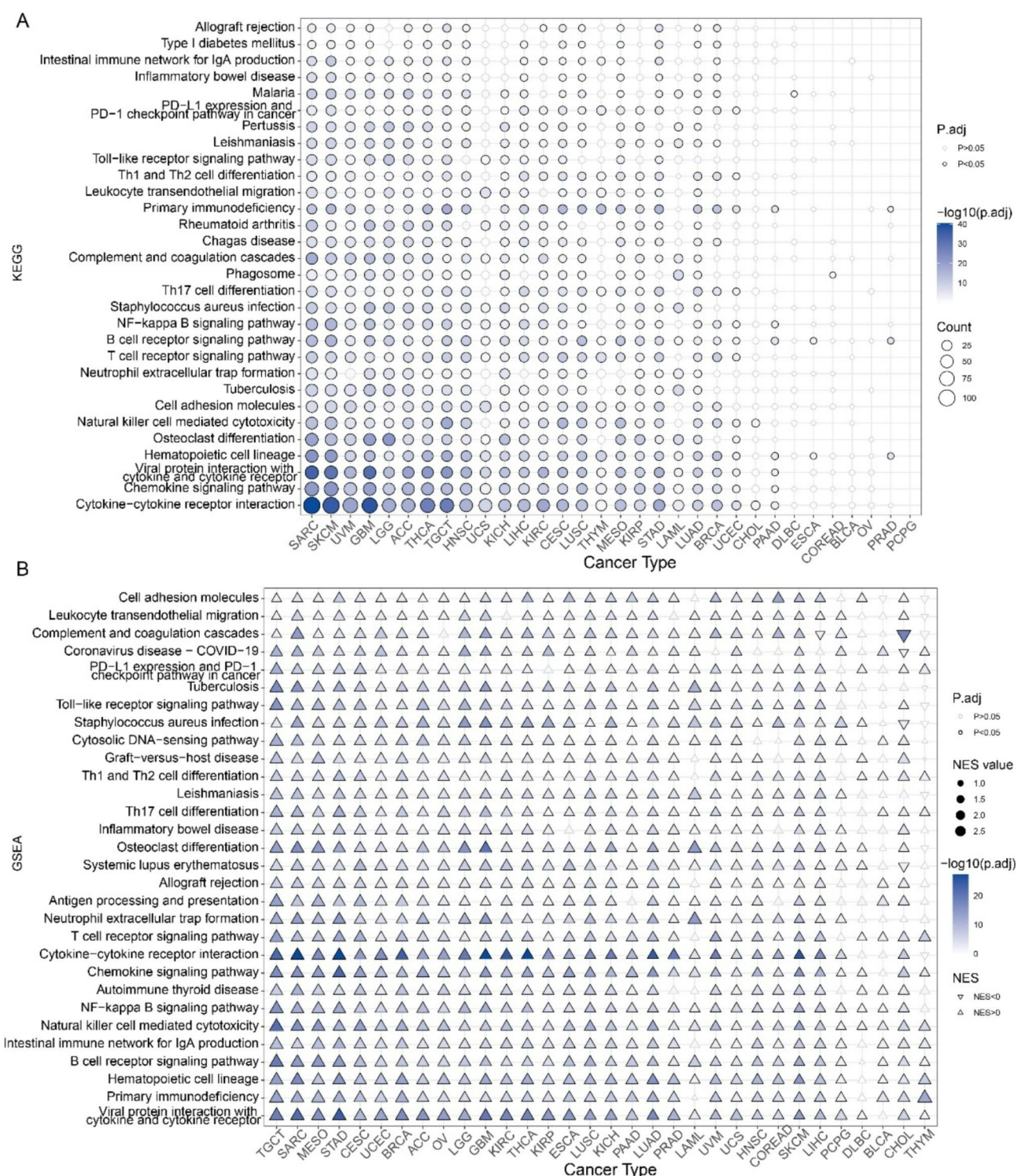


Fig. 5. Enrichment analysis of differential genes between high and low PTPN6 expression groups across cancers. (A) Bubble plot showing the results of KEGG pathway enrichment analysis for genes differentially expressed between high and low PTPN6 expression cohorts. (B) Enrichment bubble plot from Gene Set Enrichment Analysis (GSEA) depicting the pathways enriched in the high versus low PTPN6 expression groups.

The results of the GSEA enrichment analysis, shown in Fig. 5B, align closely with the KEGG results, highlighting significant enrichment across multiple immune pathways. In Supplementary Fig. 3, the results of the GO enrichment analysis are presented. Supplementary Fig. 3A reveals the enrichment of biological functions related to immune cell activation, immune cell migration, and cell proliferation. Supplementary Fig. 3B illustrates

potential molecular functions associated with PTPN6, including cytokine activation and binding, as well as immune receptor activation. Finally, Supplementary Fig. 3C provides insights into the cellular component results.

Furthermore, we utilized the STRING database to generate a PPI (Protein-Protein Interaction) network centered around PTPN6 (Fig. 6A) and conducted enrichment analysis using genes from this PPI network. Figure 6B illustrates the results of the GO enrichment analysis, highlighting significant enrichment of numerous immunological aspects such as MHC complexes, MHC activation and binding, chemokine activation, and binding of immune cell receptors. In the realm of biological functions, natural killer cells, T cell regulation and differentiation, and the JAK-STAT pathway were also enriched, aligning with our earlier findings.

Moreover, we conducted further enrichment analyses based on KEGG and REACTOME terms (Fig. 6C, D). The KEGG results reaffirmed the consistency of previous results, highlighting the enrichment of various immune pathways, particularly notable enrichment of PD-1 and PD-L1 pathway. Within the REACTOME results, several immune pathways were again identified, with multiple interleukin pathways being enriched.

Finally, we conducted a disease enrichment analysis using the GLAD4U database for the aforementioned genes, as shown in Fig. 6E. This analysis revealed the enrichment of various immune system-related diseases, with several types of leukemia featuring prominently in the results.

Single-cell analysis

Through the preceding analysis, we have uncovered a significant association between PTPN6 and immune infiltration, as well as correlations with immune-related genes, underscoring its potential role in diverse immune pathways and functions. Additionally, a consistent negative correlation between PTPN6 and tumor purity in numerous cancers suggests that tissues with elevated PTPN6 expression may contain a variety of other cell types. Therefore, To further elucidate this relationship, we conducted an in-depth analysis of 138 single-cell datasets across 45 cancer types. This analysis confirmed that PTPN6 is predominantly localized in macrophages within cancer tissues (Fig. 7A). Moreover, it is widely expressed in B cells and dendritic cells (DCs). The expression levels in CD4 + T cells and CD8 + T cells vary across different cancers.

Drug sensitive analysis

Based on enrichment analysis, the association of PTPN6 with the “PD-L1 Expression and PD-1 Checkpoint Pathway in Cancer” suggests a potential link between PTPN6, and pathways related to drug sensitivity, warranting further investigation. This led us to hypothesize that PTPN6 may exhibit correlations with other pharmaceutical agents and hold potential as an indicator for cancer therapy. Consequently, we conducted an analysis of PTPN6 expression in conjunction with various pharmaceuticals using the GSDC and CTRP databases. The results are visually represented in Fig. 8A and B, which show volcano plots depicting the correlation between drug sensitivity and PTPN6 expression levels. Our findings reveal that, for the majority of drugs, heightened PTPN6 expression is associated with increased sensitivity, suggesting that high PTPN6 expression might render these pharmaceutical agents more suitable for use. Figure 8C illustrates the intersection of the negative correlation between PTPN6 expression levels across the GSDC and CTRP databases. In total, 20 drugs in both datasets display increased sensitivity as PTPN6 expression levels rise (Fig. 8D). Among these, PAC-1, SNX-2112, BELINOSTAT, VORINOSTAT, TPCA-1, and PHA-893,888 exhibit correlations with PTPN6 in both databases that are less than -0.2 , warranting further investigation. Next, through the ToxicDB database, we observed that drugs such as Colchicine, Sulindac, and Ethionine can lead to a decrease in the expression levels of PTPN6. Conversely, drugs like 2-Bromoethylamine, Carboplatinum, and N-Nitrosodiethylamine can cause an increase in its expression, though the enhancement effect is not significant (Fig. 8E). Referring to the application of CMAP in previous research³⁵, we identified drugs related to PTPN6 by inputting associated genes into the CMAP platform (Fig. 8F). We discovered associations between PTPN6 expression and specific pharmaceutical agents. Resiquimod and felodipine showed a positive association with PTPN6 expression, suggesting potential synergy or enhanced effectiveness when combined with therapies targeting PTPN6. Conversely, BRD-K74634175 and XLOC_L2_008203 were negatively associated with PTPN6.

PTPN6 elevated expression in CRC and associated with disease staging

Given the established enrichment of PTPN6 in various cancer-related pathways and its widespread overexpression in cancer has been validated through public databases, we collected pathological samples from patients who underwent colorectal cancer surgery at our institution. The expression of PTPN6 in cancerous and adjacent tissues were assessed through immunohistochemistry (Fig. 9A). Our observations confirmed higher PTPN6 expression in cancer tissues compared to adjacent normal tissues. We then quantitatively scored the expression of PTPN6 in 20 samples using immunohistochemistry and gathered comprehensive patient data for subsequent statistical analysis. We discovered no statistically significant differences in age and gender between the high PTPN6 expression and low expression groups, though high expression patients appeared to be older. Further, T staging and TNM classification did not differ considerably between the two PTPN6 expression cohorts. Intriguingly, the data suggest high expression tumors exhibit more advanced N staging. Moreover, no distinctions in tumor volume were evident between the high and low PTPN6 expression categories (Table 1).

Knocking down PTPN6 expression inhibits the proliferation and migration of CRC cells

We further explored the expression of PTPN6 in colorectal cancer cell lines, as depicted in Fig. 9B, illustrating the protein expression across various CRC cell lines. Notably, PTPN6 exhibited minimal expression in the RKO cell line, while its highest expression was observed in the SW620 cell line, which interestingly is derived from the lymph node metastasis of SW480. Furthermore, our western blot results align with the mRNA expression trends observed in the CCLC database (Fig. 9C). Given these findings, we selected SW620 and HCT116 cell lines, which

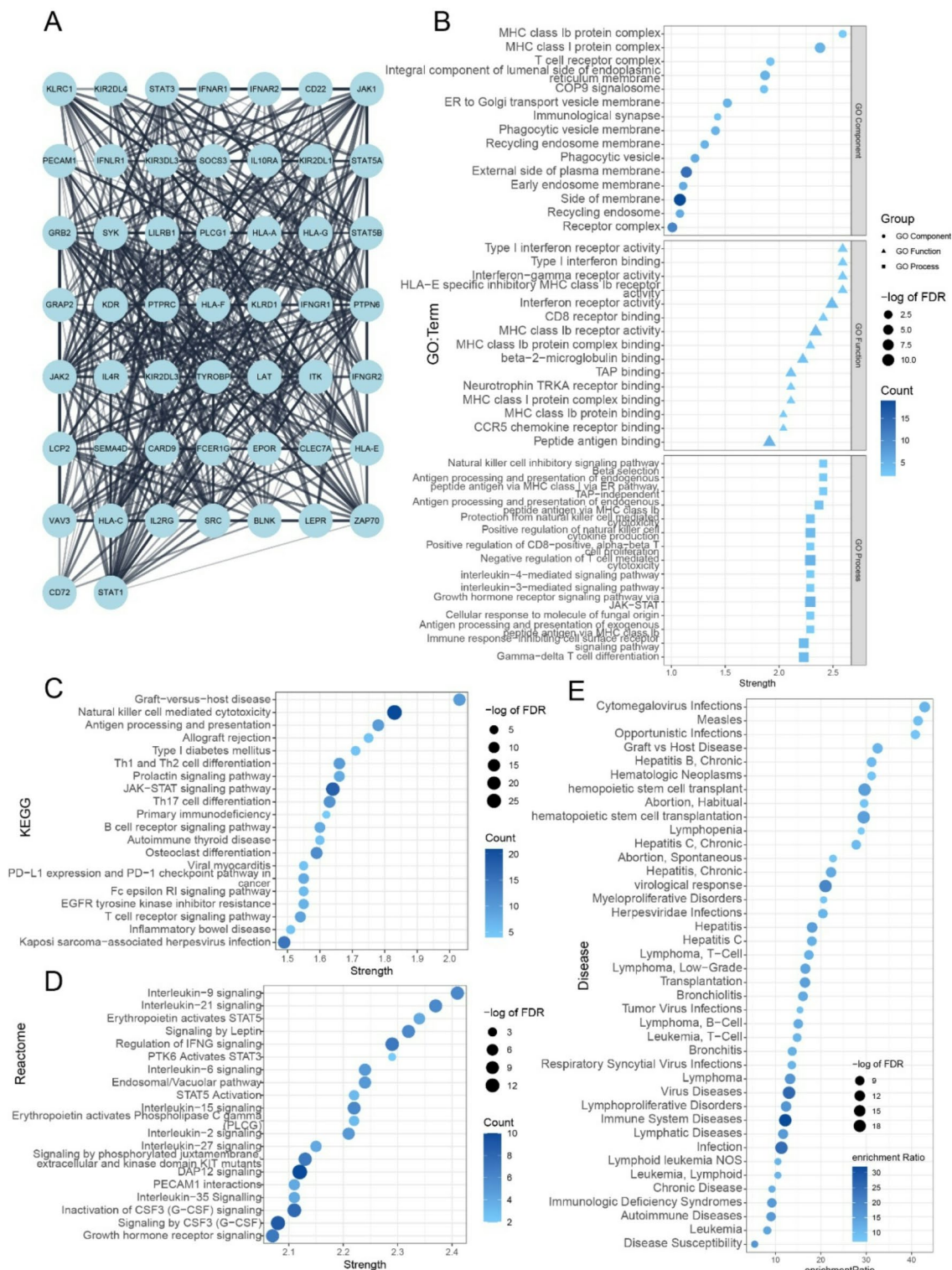


Fig. 6. PTPN6 protein-protein interaction (PPI) network and enrichment analysis. (A) PPI network of PTPN6 and its interacting partners, obtained from the STRING database. Enrichment analysis of PTPN6 PPI genes for (B) Gene Ontology (GO) terms, (C) KEGG pathways, (D) Reactome pathways; (E) Disease enrichment analysis.

exhibited the highest relative expression levels, for knockdown validation. Successful knockdown of PTPN6 was confirmed in these cell lines using siRNA (siPTPN6#1 and siPTPN6#2), with the results depicted in Fig. 9D. Subsequent functional assays examined the impact of PTPN6 knockdown on cell proliferation and migration. The results indicated a notable inhibition in proliferation trends following PTPN6 knockdown (Fig. 9E and

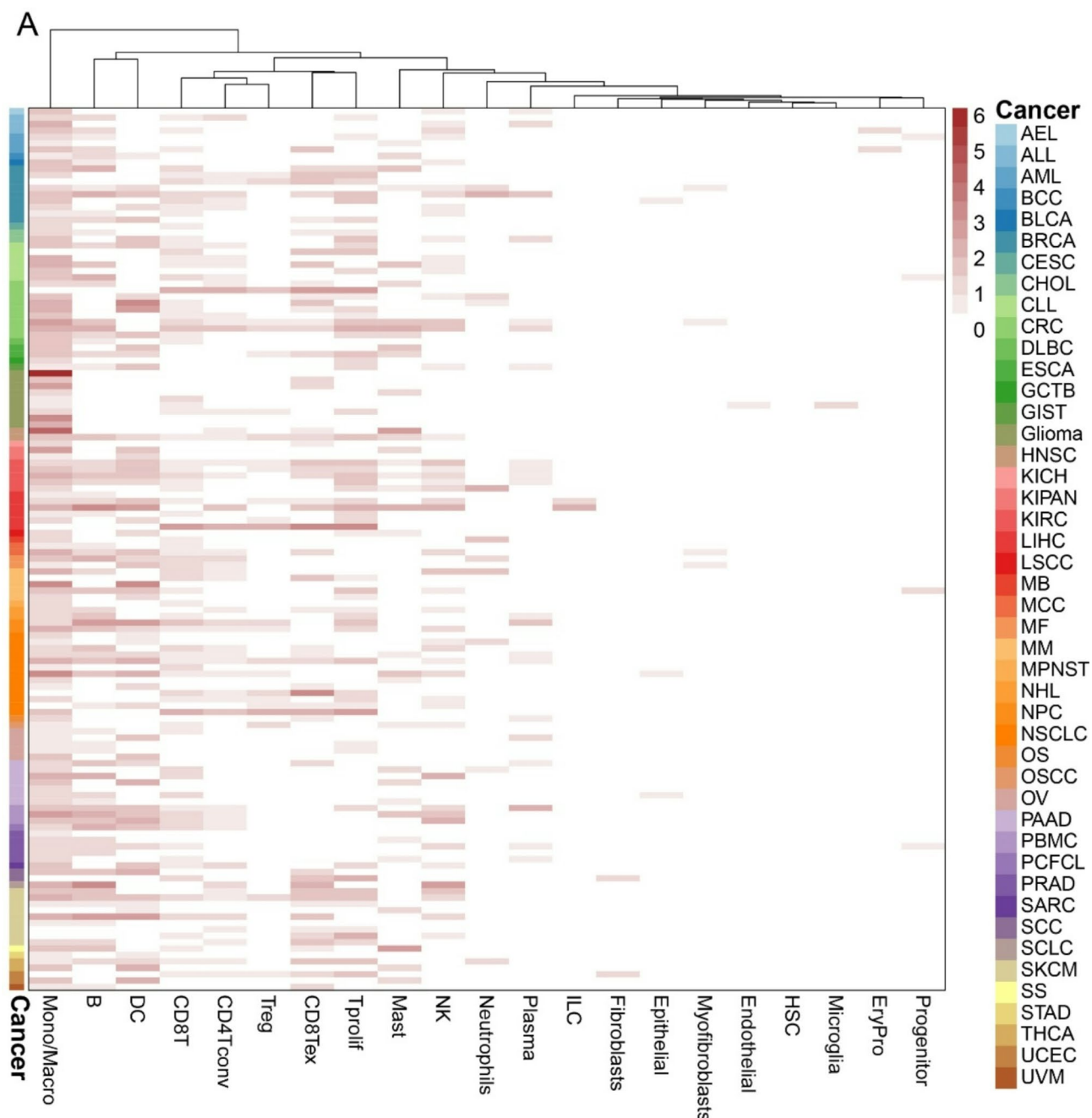


Fig. 7. PTPN6 expression across 138 single-cell datasets from the TISCH database. **(A)** Heatmap showing the relative expression levels of PTPN6 across single-cell datasets from various cancer types. The sidebar denotes cancer types and the color scale represents relative expression.

F). Furthermore, a significant reduction in the number of cell colonies was observed in the plate cloning assay (Fig. 9G). Simultaneously, cell migration was also affected, as shown in Fig. 9F. Finally, we employed immunofluorescence to validate the cellular localization of PTPN6, revealing its predominant expression in the cell nucleus (Fig. 9G). Through immunofluorescence analysis, we examined the subcellular localization of PTPN6. As shown in Fig. 9H, we found that PTPN6 is primarily localized in the nucleus.

Discussion

The data presented in this study illuminates the intricate participation of PTPN6 in oncogenesis, exhibiting varied expression phenotypes across numerous malignant neoplasms. Leveraging integration of The Cancer Genome Atlas and Genotype-Tissue Expression data, we observed meaningful variations in PTPN6 expression, underscoring a multifaceted function in tumorigenesis. Furthermore, Our results also demonstrate the prognostic significance of PTPN6 levels across multiple cancer types, challenging previous assumptions with

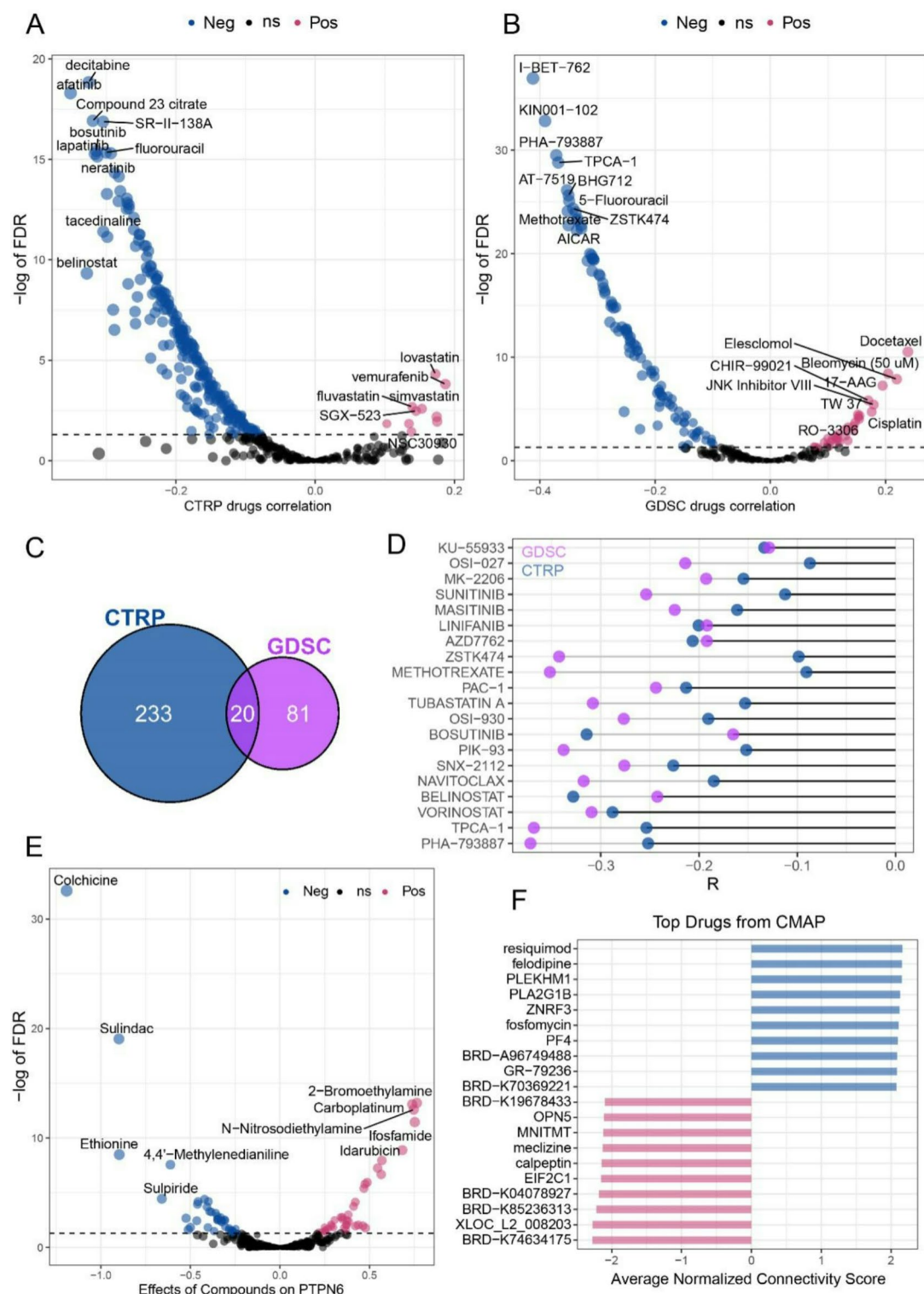
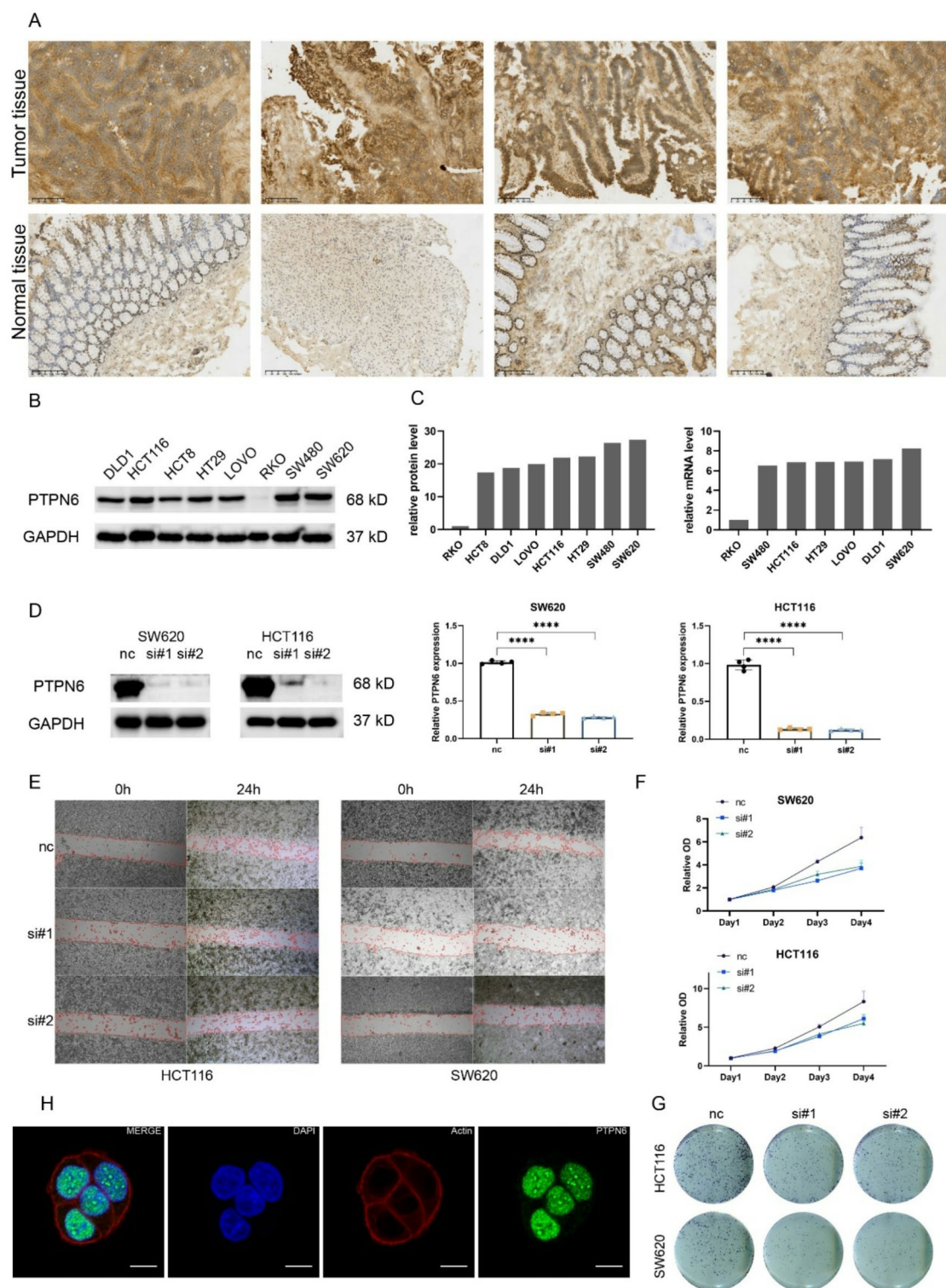


Fig. 8. Analyses of PTPN6 and drug responses. Volcano plots depicting the correlation between PTPN6 expression with drug IC₅₀ values from (A) Cancer Therapeutics Response Portal (CTRP) and (B) Genomics of Drug Sensitivity in Cancer (GDSC) databases; (C) Venn diagram showing the overlap of drugs with decreased IC₅₀ values (increased sensitivity) accompanying increased PTPN6 expression between the CTRP and GDSC datasets; (D) Details of drugs with decreased IC₅₀ accompanying increased PTPN6 expression; (E) Volcano plot showing the changes in PTPN6 expression induced by drug treatments.



findings that link higher PTPN6 expression to poorer outcomes in certain cancers. A salient facet of this study is the analysis of correlations between PTPN6 and immune genes, emphasizing its potential impact on the immune landscape of cancers.

The positive associations recognized across multiple cancers, especially in immune-related pathways, highlight PTPN6's prospective role in modulating the tumor immune microenvironment. However, exceptions identified in particular malignancies propose context-dependent operations warranting additional probing. Moreover, research has confirmed the association between PTPN6 and immune checkpoints³⁶. Another recent study found that PTPN6, when localized to the activated immune synapse, can promote NK cell tolerance in the context of MHC class I deficiency²⁶.

The correlation analysis between PTPN6 expression and immune cell infiltration along with the composition of the tumor microenvironment, provides additional insights into PTPN6's role in the complex interactions

◀**Fig. 9.** Experimental evaluation of PTPN6 in colorectal cancer (CRC) tissues and cell lines. **(A)** Immunohistochemistry images showing PTPN6 protein staining in CRC tumor tissues and normal colon sections; **(B)** Western blots of PTPN6 protein levels across CRC cell lines (Original blots are presented in Supplementary Fig. 4); **(C)** Quantitation of relative PTPN6 protein levels from the Western blots in **(B)** using ImageJ, compared to PTPN6 mRNA expression levels from the CCLE database; **(D)** Western blots and qPCR validating PTPN6 knockdown efficiency by siRNAs (Original blots are presented in Supplementary Fig. 4); **(E)** Wound healing assay images comparing siPTPN6 and control groups at 0 h and 24 h post-scratch (red dashed lines indicate scratch); **(F–G)** CCK8 and plate colony formation assays assessing impacts of PTPN6 knockdown on CRC cell proliferation; **(H)** Immunofluorescence imaging validating subcellular distribution of PTPN6 (DAPI staining in blue, F-actin in red, PTPN6 in green). White scale bar denotes ten μm. Data availability statement. The original contributions presented in the study are included in the article. Further inquiries can be directed to the corresponding author.

Characteristics	High group (n = 10)	Low group (n = 10)	P value
Age [#]	61.8 ± 10.5	53.0 ± 12.3	0.103
Sex			
Male	3	6	0.196
Female	7	4	
T stage			
T0/T1/T2	7	3	0.081
T3/T4	3	7	
N stage			
N0	6	2	0.032*
N1	3	3	
N2	1	5	
TNM stage			
Stage I	4	1	0.072
Stage II	2	1	
Stage III	4	8	
Tumor size [#]	4.26 ± 0.83	3.89 ± 0.87	0.346

Table 1. Clinical information. #Mean ± SD; **p* < 0.05.

between cancer cells and the immune system. Our findings imply PTPN6 may perform a pivotal role in governing immune responses within the tumor microenvironment, particularly in neoplasms where robust correlations are observed. This aligns with existing literature that supports the function of PTPN6 in modulating tumor immunity^{37,38}. The associations recognized in this study not only align with but also enhance our current understanding of PTPN6’s multifaceted participation in redirecting anti-tumor immunity via interactions with immune checkpoints and effector cells. Such research could uncover novel therapeutic avenues, leveraging strategic targeting of PTPN6 to enhance immune surveillance and activity specifically against malignant cells. This approach has the potential to refine and improve strategies for immune-based therapies, tailoring interventions that harness the body’s innate defense mechanisms more effectively.

Interrogation of PTPN6 genetic mutations and copy number alterations unveiled a heterogeneous landscape, underscoring the necessity for targeted approaches to decipher its function in discrete malignancies. Analysis of correlations between PTPN6 expression and key aspects of tumor biology—such as tumor heterogeneity, microsatellite instability, as well as tumor mutational burden contributes—adds complexity to our understanding of its role in oncogenesis. The interplay of PTPN6 dysregulation via multiple dimensions including expression levels, genetic, and genomic alteration underscores its extensive and multifaceted influence on neoplastic progression through a variety of mechanisms that are highly context-dependent. The comprehensive mapping of the PTPN6 somatic altered landscape alongside its transcriptional dynamics may illuminate differential functional roles across tumor types that could be strategically exploited for therapeutic benefit.

Enrichment analysis further supports the association of PTPN6’ with immune-related pathways, constituting a molecular basis for witnessed correlations within the tumor microenvironment. This analysis helps delineate how PTPN6 might influence immune evasion or activation in response to neoplastic growth. Our study highlights the nucleoplasmic localization of PTPN6, as evidenced by its nuclear staining in Fig. 9H. This aligns with its potential role in nuclear signaling, including modulation of transcription factors and chromatin-associated proteins. The PPI analysis further supports this, showing interactions with key signaling molecules like STAT1 and JAK1, which shuttle between the cytoplasm and nucleus. These interactions suggest PTPN6’s involvement in regulating nuclear phosphorylation events and transcriptional activity.

Our use of single-cell analysis single-cell has allowed for the determination of PTPN6 expression specificity across distinct immune cell subsets, thus offering a more detailed view of its functional roles at the cellular level within diverse tumor contexts. Additionally, the interaction between PTPN6 and the immune checkpoint

proteins PD-1 and PD-L1 has been corroborated by earlier studies, our in-silico analysis aligns with these findings, confirming the relevance of PTPN6 in modulating immune checkpoint pathways^{38–40}. The aggregation of multi-omics data—encompassing PTPN6 expression levels, genetic status, pathway enrichment, and single-cell localization—provides a compositely portrays of the molecular underpinnings that define PTPN6's role in modulating immune responses within the tumor microenvironment. This systems-level view corroborates and expands upon preceding evidence demonstrating PTPN6's participation in reprogramming anti-tumor immunity.

Intriguingly, our drug sensitivity analysis unveils a correlation between PTPN6 expression and efficacy of certain pharmacological compounds. This finding pioneers further exploration of PTPN6 as a prospective predictive biomarker for personalized cancer therapeutics. Through the application of Connectivity Map analysis, we identified several pharmacological agents that interact with or influence the expression and function of PTPN6. Notably, among these agents, Resiquimod—an agonist of Toll-like receptors (TLRs)—emerged as a significant drug with potential therapeutic applications⁴¹. Recent studies have highlighted Resiquimod's efficacy in the treatment of glioblastoma⁴². Resiquimod's mechanism of action primarily involves the activation of TLR7 and TLR8, which leads to the induction of a potent immune response characterized by the production of various cytokines and chemokines⁴³. These findings encourage deeper investigations into the specific interactions between Resiquimod, PTPN6, and the immune system in the context of cancer treatment.

This study bridges the gap between molecular biology and clinical outcomes by examining the effects of PTPN6 dysregulation in colorectal carcinoma. Our findings reveal a notable elevation in PTPN6 expression in CRC tissues, prominently in advanced stage disease, converges with our overarching results. Additional in vitro experiments validated the oncogenic function of PTPN6 in CRC, with PTPN6 knockdown attenuating proliferation.

In summation, our comprehensive analysis elucidates the multifaceted involvement of PTPN6 in oncogenesis, spanning from molecular interactions to clinical consequences. The context-dependent nature of PTPN6's operations underscores the necessity of tailored approaches to decode its contributions to tumorigenesis, immune modulation, and therapeutic response. However, there are limitations to this study that must be acknowledged. Firstly, the observed correlations do not establish causality, and further studies are required to validate these associations and determine the functional effects of PTPN6. Additionally, while experiments were instituted in cellular models, there was no in vivo confirmation in this study, which is regrettable. In essence, the primary aim of our research is to execute a pan-cancer systems analysis of the PTPN6 nexus, rather than focusing on its specific its mechanisms within a single type of cancer.

Moving forward, the integrative themes emerging from this study form a scaffold for a cohesive framework of PTPN6's multifaceted oncogenic and immunoregulatory roles. Additional inquiries methodically addressing the limitations of this work will further cement the rationale for therapeutically targeting PTPN6 in susceptible neoplasms. Altogether, by converged molecular, computational, experimental and clinical exploration, this study extensively portrays PTPN6 as a high-value node governing cancer progression through diverse mechanisms in a context-dependent manner. Strategic inhibition of PTPN6 signaling stands poised to impede key hallmarks across multiple cancers and reinvigorate anti-tumor immunity.

In conclusion, this pan-cancer analysis of PTPN6 revealed its multifaceted and complex involvement across diverse cancer types. Through comprehensive statistical and experimental analyses, we demonstrated that PTPN6 plays context-dependent roles, acting as both a tumor suppressor and oncogene. Of particular significance is its link to tumor immunity, as indicated by its correlations with immune pathways, immune cell infiltration, and spatial localization in immune cell subsets. The prognostic power of PTPN6 also differs amongst cancers. Crucially, our functional assays established that PTPN6 regulates proliferation in colorectal cancer cells, confirming its oncogenic role. Given PTPN6's immunomodulatory capacity and variable effects on survival, further studies should explore its potential as a biomarker or immunotherapeutic target. Overall, this systematic study expands our understanding of this protein tyrosine phosphatase's contradictory effects in cancers while spotlighting promising avenues for future research on PTPN6 in tumor immunology and precision oncology.

Method

Data collection and processing

We obtained a standardized pan-cancer dataset from the Xena functional genomics explorer (<https://xenabrowser.net/>) database. The dataset included expression data for the ENSG00000111679 (PTPN6) gene in each sample. To ensure comparability and normalization, we applied a $\log_2(x + 1)$ transformation to the expression values. To address the limitation of small sample sizes for normal tissues in the TCGA database, we also retrieved expression data for normal tissues from the GTEX database^{44,45}. Moreover, the data obtained from Xena, which has undergone batch effect correction, can be directly compared, and analyzed.

We obtained the tumor cell line expression matrix from the CCLE dataset, which is available at "<https://portals.broadinstitute.org/ccle/about>". For the statistical analysis of the CCLE data, we referenced previous study and used ANOVA to verify the statistical differences among multiple groups⁴⁶. To analyze the data, we utilized version 3.3.3 of the "ggplot2" R package^{47,48}. The correlation between PTPN6 methylation and mRNA expression across various cancer types was analyzed using the GSCA (Gene Set Cancer Analysis) platform (guolab.wchscu.cn/GSCA/)⁴⁹. The RSEM-normalized mRNA expression data and Illumina Methylation 450k level 3 data were obtained from the TCGA database. The methylation data consisted of multiple CpG sites for each gene, capturing the methylation levels at different genomic positions. To accurately assess the relationship between methylation and gene expression, we performed a correlation analysis to identify the CpG site most negatively correlated with PTPN6 mRNA expression. Spearman's correlation coefficient (R) was calculated to quantify the strength and direction of the relationship. A false discovery rate (FDR) was applied to adjust for multiple testing, ensuring

robust statistical significance. The results were visualized and summarized using the mutation module available in the GSCA platform.

Gene expression and survival analysis

Next, we acquired a high-quality prognostic dataset from the TCGA prognostic study previously conducted by Liu J et al.⁵⁰. The Cox proportional hazards regression model was then built using the `coxph` function of the “survival” R package (version 3.2–7) to analyze the relationship between gene expression and prognosis in each tumor. Univariate Cox regression analysis and forest plots generated through the “forestplot” R package were used to display the P value, HR, and 95% CI of each variable. The relationship between methylation and survival was analyzed using MethSurv tool⁵¹. This valuable online website allows for the preliminary evaluation of cancer biomarkers based on gene methylation data.

Genetic heterogeneity analysis

We obtained Homologous recombination deficiency (HRD) and the microsatellite instability (MSI) data from previous studies and merged this data with PTPN6 expression levels for correlation analysis^{52,53}. For TMB and MATH, we utilized the R package “maftools” (version 2.8.05) to calculate the values and then performed correlation analysis with PTPN6 expression levels⁵⁴. Tumor purity was determined using the ABSOLUTE algorithm, as provided by the TCGA Research Network^{55,56}.

Immune analysis

We extracted the expression data of two types of immune checkpoint pathway genes (inhibitory and stimulatory) as well as five types of immune pathway genes (chemokine, receptor, MHC, immuno-inhibitor, and immuno-stimulator) from the downloaded TCGA dataset. To ensure the accuracy of our analysis, we filtered out all normal samples, focusing solely on tumor samples. Furthermore, we utilized the `deconvolve` method from the R package IOBR (version 0.99.9) to explore the relationship between immune cells and the expression of PTPN6^{57,58}.

Notably, the ESTIMATE algorithm includes three scores: immune score (assessment of immune cell infiltration level); stromal score (assessment of immunity of stromal components); and ESTIMATE score. The “Estimate” R package is used to evaluate the above three scores for each TCGA sample⁵⁹. To ensure statistical accuracy, we used the false discovery rate (FDR) method to correct the p-values when performing the correlation analysis.

Protein–protein interaction analysis

The protein-protein interaction (PPI) network was established using the Search Tool for the Retrieval of Interacting Genes (STRING) (<https://cn.string-db.org/>) with the following input parameters: “evidence”, “experiments”, and “low confidence level”. A total of 51 nodes were finally obtained, which were then subjected to enrichment analysis.

Enrichment analysis

We performed enrichment analysis using the R package “clusterProfiler” for GO, KEGG, and GSEA analyses^{60–63}. For genes obtained through PPI, we conducted KEGG and GO enrichment analyses. In each cancer type of TCGA data, we divided the samples into high expression and low expression groups based on PTPN6 expression levels. We then used the R package “limma” for differential analysis. Genes with fold change (FC) ≥ 2 and p-value < 0.05 were selected for KEGG and GO enrichment analysis⁶⁴. Subsequently, GSEA enrichment analysis was performed based on FC rankings, using KEGG as the keyType for GSEA analysis. Disease enrichment analysis was performed using the GLAD4U databases⁶⁵.

Single-cell analysis

The Tumor Immune Single Cell Hub 2 (TISCH2) serves as a valuable repository of single-cell RNA-seq (scRNA-seq) data derived from both human and mouse tumors⁶⁶. This resource facilitates an in-depth exploration and analysis of gene expression patterns within the tumor microenvironment (TME) across various cancer types. We obtained 138 single-cell datasets encompassing 45 types of cancer from the TISCH2 database. After downloading the expression data for PTPN6 in different cell types from these 138 datasets, we utilized R language to create a heatmap.

Drug sensitivity analysis

For drug sensitivity analysis, we utilized two databases: the Genomics of Drug Sensitivity in Cancer (GDSC) database (<https://www.cancerrxgene.org/>) and the Cancer Therapeutics Response Portal (CTRP) database (<https://portals.broadinstitute.org/ctrp/>)^{67–72}. In both databases, we extracted the expression data and drug sensitivity information for each cell line. Subsequently, we conducted correlation analysis between gene expression and drug sensitivity. Furthermore, we conducted an analysis of the impact of various drugs on PTPN6 expression using the ToxicodB database (<https://www.toxicodb.ca/>). The database provided information on changes in PTPN6 expression levels following different drug treatments, with parameters “High Dose” and “Select Time 24.” The Connectivity Map (CMAP) is a powerful tool used to explore the potential relationships between diseases, genetic expression, and small molecule drugs^{73,74}. Using the CMAP, we input genes associated with PTPN6 into the platform to identify potential therapeutic drugs.

Cell culture

The present study used eight cell lines for in vitro experiments. Two colorectal cancer cell lines (SW620 and HCT116) are included. SW620 cells were grown in 10% FBS-supplemented DMEM media. HCT116 was grown on McCoy's 5 A medium supplemented with 10% FBS. The cultures were incubated at 37 °C with 5% CO₂. The human colorectal cancer cell lines SW620 and HCT116 were procured from the Meisen Cell (China).

Cell viability assay and plate colony formation assay

CKK-8 Cell Counting Kit (A311-01) was obtained from VAZYME (www.VAZYME.com/) for the purpose of conducting the proliferative assay. The experimental protocol was followed as per the instructions provided by the manufacturer. The absorbance at 450 nm was measured using a microplate reader from Tecan, Switzerland.

For plate colony formation assay, cells were harvested via enzymatic digestion, centrifuged, resuspended in culture medium and quantified with Countess 3 Automated Cell Counter (Invitrogen). One thousand viable cells were seeded per well into 6-well cell culture plates, which were maintained at 37 °C in a humidified 5% CO₂ incubator. Following 2 weeks of incubation allowing for colony formation, culture medium was removed, and cell colonies were fixed with methanol for 60 min and stained with 0.1% crystal violet solution for 30 min. Plates were washed, air dried, photographed and colonies enumerated.

Wound healing assay

For the wound healing assay, cells were seeded in 6-well plates and cultured until confluence reached 90%. Three vertical scratches were introduced in each well, and cell debris was removed with PBS to clearly visualize the areas. Cells continued growing for 24 h in serum-free media before removing the media again and capturing images per the protocol.

Total RNA extraction and qRT-PCR

FastPure Cell/Tissue Total RNA Isolation Kit V2 (RC112) from VAZYME used to extract RNA from cell. HiScript II Q RT SuperMix for qPCR (+gDNA wiper) (R223) from VAZYME used to reverse transcription. ChamQ Universal SYBR qPCR Master Mix (Q711) from VAZYME used to qPCR validation.

Primer of PTPN6 sequences (5'→3'): F: GCCTGGACTGTGACATTGAC, R: ATGTTCCCGTACTCCGAC TC.

Primer of GAPDH sequences (5'→3'): CAGGAGGCATTGCTGATGAT, R: GAAGGCTGGGGCTCATTT.

Cell transfects

siRNA transfect was performed using Lipofectamine 2000 reagent (INVITROGEN) according to the manufacturer's instruction. siRNA-1 sequences: Sense: 5'-GAGCAUGACACAACCGAAUTT-3', Antisense: 5'-AUUCGGUUGUGUCAUGCUCTT-3'. siRNA-2 sequences: Sense: 5'-GCCCAGUUCAUUGAAACCATT-3', Antisense: 5'-UGGUUCAAUGAACUGGGCTT-3'; siRNA-3 sequences: Sense: 5'-GAGACUUCGUGCUUU CUGUTT-3', Antisense: 5'-ACAGAAAGCACGAAGUCUCTT-3.

Immunofluorescence assay

Immunofluorescence staining was performed using an antibody from ABCAM (ab124942) following the protocol (<https://www.abcam.cn/protocols/immunocytochemistry-immunofluorescence-protocol>). First, SW620 cells were transferred to confocal culture dishes and cultured until approximately 60% confluent. The cells then underwent blocking and permeabilization, followed by incubation with the antibody diluted 1:500. An Alexa Fluor 488 secondary antibody kit (P0176) from BEYOTIME was used for secondary antibody binding. F-actin staining was then conducted using BEYOTIME's Actin-Tracker Red 555 (C2203S) to visualize microfilaments. Finally, cell nuclei were stained using INVITROGEN's DAPI (D3571). After staining, images were captured using a NIKON Confocal Microscope (A1RHD25).

Immunohistochemical staining (IHC) assay and patient samples

Tissue specimens were collected from colorectal cancer patients undergoing surgical resection at the Department of Colorectal Surgery of Zhejiang Cancer Hospital, procuring a total of 20 matched tumor and adjacent normal pairs. This study was evaluated and approved by the Ethics Committee of Zhejiang Cancer Hospital, with all procedures performed per the Declaration of Helsinki (1964) and subsequent amendments. Written informed consent was obtained from all subjects and/or their legal guardian(s). The PTPN6 antibody utilized was commercially sourced from ABCAM (catalog number ab124942). The specific methodology for the immunohistochemistry follows our previously published work⁷⁵. Following immunohistochemical scoring and grouping of 20 samples, high and low expression groups were compared via Student's t-test or nonparametric tests with regards to age, gender, T stage, N stage, TNM stage, and tumor size.

Western blots assay

Western blot analysis was instituted to evaluate PTPN6 protein expression across cell lines. Total protein was extracted from cultured cells using RIPA lysis buffer (BEYOTIME, P0013B) containing protease and phosphatase inhibitors. Equivalent protein amounts were resolved by SDS-PAGE and transferred to PVDF membranes. Membranes were blocked and probed with primary antibodies targeting PTPN6 and GAPDH (CELL SIGNALING TECHNOLOGY, 14C10), followed by HRP-conjugated secondary antibodies and ECL-based detection.

Data availability

The original contributions presented in the study are included in the article. Further inquiries can be directed to the corresponding author.

Received: 2 January 2024; Accepted: 27 March 2025

Published online: 01 April 2025

References

- Kiratikanon, S., Chattipakorn, S. C., Chattipakorn, N. & Kumfu, S. The regulatory effects of PTPN6 on inflammatory process: Reports from mice to men. *Arch. Biochem. Biophys.* **721**, 109189. <https://doi.org/10.1016/j.abb.2022.109189> (2022).
- Speir, M. et al. Ptpn6 inhibits caspase-8- and Ripk3/Mlkl-dependent inflammation. *Nat. Immunol.* **21**, 54–64. <https://doi.org/10.1038/s41590-019-0550-7> (2020).
- Jiang, J. et al. Platelet ITGA2B inhibits caspase-8 and Rip3/Mlkl-dependent platelet death though PTPN6 during sepsis. *iScience* **26**, 107414. <https://doi.org/10.1016/j.isci.2023.107414> (2023).
- Lukens, J. R. et al. RIP1-driven autoinflammation targets IL-1 α independently of inflammasomes and RIP3. *Nature* **498**, 224–227. <https://doi.org/10.1038/nature12174> (2013).
- Demosthenous, C., Han, J. J., Hu, G., Stenson, M. & Gupta, M. Loss of function mutations in PTPN6 promote STAT3 deregulation via JAK3 kinase in diffuse large B-cell lymphoma. *Oncotarget* **6**, 44703 (2015).
- Fang, H., Ma, W., Guo, X. & Wang, J. PTPN6 promotes chemosensitivity of colorectal cancer cells via inhibiting the SP1/MAPK signalling pathway. *Cell Biochem. Funct.* **39**, 392–400 (2021).
- Varone, A., Spano, D. & Corda, D. Shp1 in solid cancers and their therapy. *Front. Oncol.* **10**, 935 (2020).
- Banville, D., Stocco, R. & Shen, S. H. Human protein tyrosine phosphatase 1 C (PTPN6) gene structure: Alternate promoter usage and exon skipping generate multiple transcripts. *Genomics* **27**, 165–173 (1995).
- Jones, M. L., Craik, J. D., Gibbins, J. M. & Poole, A. W. Regulation of SHP-1 tyrosine phosphatase in human platelets by Serine phosphorylation at its C terminus**. *J. Biol. Chem.* **279**, 40475–40483. <https://doi.org/10.1074/jbc.M402970200> (2004).
- Abram, C. L. & Lowell, C. A. Shp1 function in myeloid cells. *J. Leukoc. Biol.* **102**, 657–675. <https://doi.org/10.1189/jlb.2MR0317-105R> (2017).
- Youssef, G. et al. The presence of Y674/Y675 phosphorylated NTRK1 via TP53 repression of PTPN6 expression as a potential prognostic marker in neuroblastoma. *Hum. Pathol.* **86**, 182–192. <https://doi.org/10.1016/j.humpath.2018.12.003> (2019).
- Zhang, X. et al. Research on the epigenetic regulation mechanism of the PTPN6 gene in advanced chronic myeloid leukaemia. *Br. J. Haematol.* **178**, 728–738. <https://doi.org/10.1111/bjh.14739> (2017).
- Demosthenous, C., Han, J. J., Hu, G., Stenson, M. & Gupta, M. Loss of function mutations in PTPN6 promote STAT3 deregulation via JAK3 kinase in diffuse large B-cell lymphoma. *Oncotarget* **6**, 44703–44713. <https://doi.org/10.18632/oncotarget.6300> (2015).
- Mok, S. C., Kwok, T. T., Berkowitz, R. S., Barrett, A. J. & Tsui, F. W. Overexpression of the protein tyrosine phosphatase, nonreceptor type 6 (PTPN6), in human epithelial ovarian cancer. *Gynecol. Oncol.* **57**, 299–303. <https://doi.org/10.1006/gyno.1995.1146> (1995).
- Liu, G. et al. PTPN6-EGFR protein complex: A novel target for colon cancer metastasis. *J. Oncol.* **2022**, 7391069. <https://doi.org/10.1155/2022/7391069> (2022).
- Fang, H., Ma, W., Guo, X. & Wang, J. PTPN6 promotes chemosensitivity of colorectal cancer cells via inhibiting the SP1/MAPK signalling pathway. *Cell Biochem. Funct.* **39**, 392–400. <https://doi.org/10.1002/cbf.3604> (2021).
- Zhang, X. et al. Single-cell and bulk sequencing analyses reveal the immune suppressive role of PTPN6 in glioblastoma. *Aging* **15**, 9822–9841. <https://doi.org/10.18632/aging.205052> (2023).
- Geng, Q., Xian, R., Yu, Y., Chen, F. & Li, R. SHP-1 acts as a tumor suppressor by interacting with EGFR and predicts the prognosis of human breast cancer. *Cancer Biol. Med.* **19**, 468–485. <https://doi.org/10.20892/j.issn.2095-3941.2020.0501> (2021).
- Liu, C. Y. et al. Sequential combination of docetaxel with a SHP-1 agonist enhanced suppression of p-STAT3 signaling and apoptosis in triple negative breast cancer cells. *J. Mol. Med.* **95**, 965–975. <https://doi.org/10.1007/s00109-017-1549-x> (2017).
- Fan, L. C. et al. SHP-1 is a negative regulator of epithelial-mesenchymal transition in hepatocellular carcinoma. *Oncogene* **34**, 5252–5263. <https://doi.org/10.1038/onc.2014.445> (2015).
- Wei, Q., Luo, S. & He, G. Mechanism study of tyrosine phosphatase shp-1 in inhibiting hepatocellular carcinoma progression by regulating the SHP2/GM-CSF pathway in TAMs. *Sci. Rep.* **14**, 9128. <https://doi.org/10.1038/s41598-024-59725-w> (2024).
- Chi, D. et al. CLEC12B suppresses lung cancer progression by inducing SHP-1 expression and inactivating the PI3K/AKT signaling pathway. *Exp. Cell Res.* **409**, 112914. <https://doi.org/10.1016/j.yexcr.2021.112914> (2021).
- Cao, R. et al. SHP1-mediated cell cycle redistribution inhibits radiosensitivity of non-small cell lung cancer. *Radiation Oncol.* **8**, 178. <https://doi.org/10.1186/1748-717x-8-178> (2013).
- Ye, F. et al. TGF- β antagonizes IFN- γ -mediated adaptive immune evasion via activation of the AKT-Smad3-SHP1 axis in lung adenocarcinoma. *Cancer Res.* <https://doi.org/10.1158/0008-5472.Can-22-3009> (2023).
- Carmi, Y. et al. Akt and SHP-1 are DC-intrinsic checkpoints for tumor immunity. *JCI Insight* **1**, e89020. <https://doi.org/10.1172/jci.insight.89020> (2016).
- Schmied, L. et al. SHP-1 localization to the activating immune synapse promotes NK cell tolerance in MHC class I deficiency. *Sci. Signal.* **16**, eabq0752. <https://doi.org/10.1126/scisignal.abq0752> (2023).
- Liu, C. Y. et al. The tyrosine kinase inhibitor nintedanib activates SHP-1 and induces apoptosis in triple-negative breast cancer cells. *Exp. Mol. Med.* **49**, e366. <https://doi.org/10.1038/emmm.2017.114> (2017).
- Wang, C. C. et al. Novel potential therapeutic targets of PTPN families for lung cancer. *J. Personalized Med.* **12**, 1947 (2022).
- Anuraga, G. et al. Potential prognostic biomarkers of NIMA (Never in mitosis, gene A)-related kinase (NEK) family members in breast cancer. *J. Pers. Med.* **11**. <https://doi.org/10.3390/jpm11111089> (2021).
- Zhang, X. et al. Single-cell and bulk sequencing analyses reveal the immune suppressive role of PTPN6 in glioblastoma. *Aging* **15**, 9822 (2023).
- Spalinger, M. R., McCole, D. F., Rogler, G. & Scharl, M. Role of protein tyrosine phosphatases in regulating the immune system: Implications for chronic intestinal inflammation. *Inflamm. Bowel Dis.* **21**, 645–655 (2015).
- Nagarsheth, N., Wicha, M. S. & Zou, W. Chemokines in the cancer microenvironment and their relevance in cancer immunotherapy. *Nat. Rev. Immunol.* **17**, 559–572. <https://doi.org/10.1038/nri.2017.49> (2017).
- Ribas, A. & Wolchok, J. D. Cancer immunotherapy using checkpoint blockade. *Science* **359**, 1350–. <https://doi.org/10.1126/science.aar4060> (2018).
- Pardoll, D. M. The blockade of immune checkpoints in cancer immunotherapy. *Nat. Rev. Cancer* **12**, 252–264. <https://doi.org/10.1038/nrc3239> (2012).
- Wang, C. Y. et al. Gene signatures and potential therapeutic targets of amino acid metabolism in estrogen receptor-positive breast cancer. *Am. J. Cancer Res.* **10**, 95–113 (2020).
- Snook, J. P., Soedel, A. J., Ekiz, H. A., O'Connell, R. M. & Williams, M. A. Inhibition of SHP-1 expands the repertoire of antitumor T cells available to respond to immune checkpoint blockade. *Cancer Immunol. Res.* **8**, 506–517. <https://doi.org/10.1158/2326-6066.Cir-19-0690> (2020).

Author contributions

YC.Z. contributions to the conception, design of the work, drafted the work, acquisition and analysis data; WY.Z. contributions to the drafted the work, in vitro experiments and analysis data; CJ.Z., H.Z., CL.W., contributions to in vitro experiments and analysis data; HY.W., ZM.Y. and J.L. contributions to analysis data, W.M., HY.F., Q.Z., HX.J. and GY.W. provided funding, reviewed the manuscript, and approved the study.

Declarations

Competing interests

The authors declare no competing interests.

Additional information

Supplementary Information The online version contains supplementary material available at <https://doi.org/10.1038/s41598-025-96302-1>.

Correspondence and requests for materials should be addressed to Q.Z., H.J. or G.W.

Reprints and permissions information is available at www.nature.com/reprints.

Publisher's note Springer Nature remains neutral with regard to jurisdictional claims in published maps and institutional affiliations.

Open Access This article is licensed under a Creative Commons Attribution-NonCommercial-NoDerivatives 4.0 International License, which permits any non-commercial use, sharing, distribution and reproduction in any medium or format, as long as you give appropriate credit to the original author(s) and the source, provide a link to the Creative Commons licence, and indicate if you modified the licensed material. You do not have permission under this licence to share adapted material derived from this article or parts of it. The images or other third party material in this article are included in the article's Creative Commons licence, unless indicated otherwise in a credit line to the material. If material is not included in the article's Creative Commons licence and your intended use is not permitted by statutory regulation or exceeds the permitted use, you will need to obtain permission directly from the copyright holder. To view a copy of this licence, visit <http://creativecommons.org/licenses/by-nc-nd/4.0/>.

© The Author(s) 2025